



Published in final edited form as:

J Invest Dermatol. 2016 January ; 136(1): 342–344. doi:10.1038/JID.2015.371.

Diabetic wounds exhibit distinct microstructural and metabolic heterogeneity through label-free multiphoton microscopy

Kyle P. Quinn¹, Ermelindo C. Leal², Ana Tellechea², Antonios Kafanas², Michael E. Auster², Aristidis Veves², and Irene Georgakoudi¹

¹Department of Biomedical Engineering, Tufts University, Medford, MA, 02155 USA

²Beth Israel Deaconess Medical Center, Boston, MA, 02215 USA

TO THE EDITOR

Cutaneous wound healing is a complex process requiring the coordination of inflammatory cells, endothelial cells, fibroblasts, and keratinocytes (Gurtner *et al.*, 2008). Chronic wounds fail to progress through this coordinated process, and are often characterized by prolonged inflammation, poor vascularization, callus formation, and infection (Brem *et al.*, 2007; Martin *et al.*, 2010). A wide variety of advanced wound care products have been developed to target specific characteristics of chronic wounds (Apelqvist, 2012). However, no single therapy has yielded widespread clinical success, and there is a critical need to develop new biomarkers and diagnostic technologies to evaluate wound status and guide care.

Currently, wound closure is the only accepted objective endpoint to evaluate wound treatments, and there is a lack of quantitative surrogate biomarkers to predict healing at earlier stages. Multi-photon microscopy techniques, such as two-photon excited fluorescence (TPEF), have emerged as useful approaches to evaluate epithelial tissues and offer advantages in imaging depths and signal collection over confocal microscopy (Balu *et al.*, 2013; Varone *et al.*, 2014). Through TPEF imaging, the intrinsic fluorescence of nicotinamide and flavin adenine dinucleotides (NADH and FAD) can be measured without the application of exogenous stains (Georgakoudi and Quinn, 2012; Zipfel *et al.*, 2003). An optical redox ratio of FAD/(NADH+FAD) autofluorescence has been computed from a variety of cells and tissues and is correlated with the intracellular concentration ratio of NAD⁺/NADH (Quinn *et al.*, 2013; Varone *et al.*, 2014). This non-invasive measure of the relative rates of glucose catabolism to oxidative phosphorylation has been used to help diagnose disease and evaluate tissue development (Georgakoudi and Quinn, 2012).

Although metabolic stress at the systemic and tissue level often coincides with chronicity, the dynamics of metabolism in the wound at the cellular level are not well understood.

Users may view, print, copy, and download text and data-mine the content in such documents, for the purposes of academic research, subject always to the full Conditions of use:http://www.nature.com/authors/editorial_policies/license.html#terms

Correspondence: Kyle Quinn, PhD, Department of Biomedical Engineering, University of Arkansas, 120 John A. White, Jr. Engineering Hall, Fayetteville, AR 72701, USA, kyle@quinnlab.org, 608-347-8890 (phone), 479-575-4346 (fax).

CONFLICT OF INTEREST

The authors state no conflict of interest.

Using label-free multi-photon microscopy, the objective of this study was to provide an initial quantitative assessment of metabolic biomarkers with sensitivity to differences between non-diabetic and diabetic wounds. To this end, multiphoton imaging was performed on unstained sections of full-thickness excisional wounds from the dorsum of a streptozotocin (STZ)-induced diabetic mouse model. Animal studies were conducted in accordance with Beth Israel Deaconess Medical Center IACUC protocol #072-2012 and Tufts IACUC protocol #M2014-58. Additional methods details can be found in Supplementary Material.

The use of endogenous TPEF imaging enables a clear visualization and discrimination of distinct wound regions, similar to histopathology (Fig. 1, Supplementary Figs. 1–2). The simultaneous collection of second harmonic generation (SHG) images also can provide sensitivity to fibrillar collagen, helping delineate the dermal layer (Supplementary Fig. 1). Upon isolating NADH and FAD fluorescence (Supplementary Material) and computing a redox ratio of $FAD/(NADH + FAD)$ on a pixel-by-pixel basis, distinct local differences in metabolism are evident (Fig. 1). At Day 0 (unwounded tissue), redox ratio maps do not clearly delineate the epidermis and dermis (Fig. 1a, e). However, at Day 3 post-wounding, a hyperplastic epidermis is evident at the wound edge with a significantly lower redox ratio ($p < 0.0001$) relative to Day 0 and other surrounding tissue regions (Fig. 1b, f, h). The non-diabetic epithelial tongue demonstrates a gradient of increasing redox ratio values from the thick proliferative base to the migrating tip at Day 3 (Fig. 1b). This spatial pattern and the significant increases ($p = 0.0241$) in the non-diabetic epithelial redox ratio (Fig. 1h) by Day 10 indicate sensitivity to a shift from an anabolic proliferative phase to a migratory phase driven by ATP-dependent actin reorganization (Pollard and Borisy, 2003).

In contrast to normal wound healing, the redox ratio of the epidermis in diabetic wound edges remains significantly lower than non-diabetic controls at Day 10 ($p = 0.0410$) (Fig. 1g, h), which is consistent with the sustained hyperproliferation of keratinocytes and lack of migration by the non-healing edge found in many chronic wounds (Brem *et al.*, 2007). These findings are further supported by the significant correlation between epidermis redox ratio and thickness ($\rho = -0.563$, $p = 0.0079$), and indicate that TPEF imaging can provide early identification of keratinocyte dysfunction during re-epithelialization. Additionally, the epidermis redox ratio is negatively correlated with neutrophil accumulation and blood vessel density (Table S1). Aside from distinct spatiotemporal patterns of cell metabolism between diabetic and non-diabetic wounds, an overall lower optical redox ratio was detected in diabetic mice ($p = 0.0037$) compared to non-diabetic controls. Both hypoxia and increased glucose catabolism have been associated with low redox ratios and may explain this overall difference (Georgakoudi and Quinn, 2012; Mayevsky and Rogatsky, 2007). However, additional work is necessary to evaluate the fluorescence contribution of advanced glycation end products or other fluorophores present in skin (Kollias *et al.*, 1998).

The granulation tissue within the wound exhibits a significantly higher redox ratio ($p < 0.0001$) than the epidermis (Fig. 1b, c, f, g) that is correlated with neutrophil accumulation ($\rho = 0.5639$, $p = 0.0357$), blood vessel density ($\rho = -0.608$, $p = 0.0212$), and spindle cell count ($\rho = -0.684$, $p = 0.007$) (Table S1). In the granulation tissue, potential significant energy demands requiring NADH oxidation include the migration of

inflammatory cells and fibroblasts, the production of reactive oxygen species, and phagocytosis (Kominsky *et al.*, 2010). Furthermore, NADH production may also be inhibited by the presence of reactive oxygen species (Rojkind *et al.*, 2002), driving the redox ratio even higher. The distinct contrast between the metabolism of the epithelium and underlying granulation tissue and stroma suggests high-resolution, depth-resolved imaging techniques are necessary to accurately characterize wound metabolism.

In summary, we demonstrate label-free multiphoton imaging can characterize the unique metabolic requirements of different wound regions (Fig. 1). Although the current study focused on identifying potential optical biomarkers using unstained tissue cryosections, it is feasible to non-invasively acquire depth-resolved images of NADH, FAD, and collagen from wounds *in vivo* (Supplementary Figure 2). Future work will explore the ability of TPEF to non-invasively characterize dynamic changes in diabetic wound metabolism *in vivo* and assess different therapies. As label-free multiphoton microscopy becomes more common in the clinic (Balu *et al.*, 2013; Konig *et al.*, 2007), the continued development and validation of these quantitative metabolic biomarkers could enable the real-time, non-invasive detection and characterization of delayed wound healing.

Supplementary Material

Refer to Web version on PubMed Central for supplementary material.

Acknowledgments

This research was supported by National Institutes of Health Grant Numbers K99EB017723 (KPQ), F32AR061933 (KPQ), R01EB007542 (IG), and R01NS066205 (AV), as well as American Cancer Society Grant RSG-09-174-01-CCE (IG).

Abbreviations used

NADH	Nicotinamide adenine dinucleotide
FAD	Flavin adenine dinucleotide
TPEF	two-photon excited fluorescence
SHG	second harmonic generation
PMT	photomultiplier tube
ROI	region of interest
STZ	streptozotocin

References

- Apelqvist J. Diagnostics and treatment of the diabetic foot. *Endocrine*. 2012; 41:384–97. [PubMed: 22367583]
- Balu M, Mazhar A, Hayakawa CK, et al. In Vivo Multiphoton NADH Fluorescence Reveals Depth-Dependent Keratinocyte Metabolism in Human Skin. *Biophys J*. 2013; 104:258–67. [PubMed: 23332078]

- Brem H, Stojadinovic O, Diegelmann RF, et al. Molecular markers in patients with chronic wounds to guide surgical debridement. *Molecular medicine*. 2007; 13:30–9. [PubMed: 17515955]
- Georgakoudi I, Quinn KP. Optical Imaging Using Endogenous Contrast to Assess Metabolic State. *Annu Rev Biomed Eng*. 2012; 14:351–67. [PubMed: 22607264]
- Gurtner GC, Werner S, Barrandon Y, et al. Wound repair and regeneration. *Nature*. 2008; 453:314–21. [PubMed: 18480812]
- Kollias N, Gillies R, Moran M, et al. Endogenous skin fluorescence includes bands that may serve as quantitative markers of aging and photoaging. *J Invest Dermatol*. 1998; 111:776–80. [PubMed: 9804337]
- Kominsky DJ, Campbell EL, Colgan SP. Metabolic shifts in immunity and inflammation. *J Immunol*. 2010; 184:4062–8. [PubMed: 20368286]
- Konig K, Ehlers A, Riemann I, et al. Clinical two-photon microendoscopy. *Microsc Res Tech*. 2007; 70:398–402. [PubMed: 17393493]
- Martin JM, Zenilman JM, Lazarus GS. Molecular microbiology: new dimensions for cutaneous biology and wound healing. *J Invest Dermatol*. 2010; 130:38–48. [PubMed: 19626034]
- Mayevsky A, Rogatsky GG. Mitochondrial function in vivo evaluated by NADH fluorescence: from animal models to human studies. *Am J Physiol Cell Physiol*. 2007; 292:C615–40. [PubMed: 16943239]
- Pollard TD, Borisy GG. Cellular motility driven by assembly and disassembly of actin filaments. *Cell*. 2003; 112:453–65. [PubMed: 12600310]
- Quinn KP, Sridharan GV, Hayden RS, et al. Quantitative metabolic imaging using endogenous fluorescence to detect stem cell differentiation. *Scientific reports*. 2013; 3:3432. [PubMed: 24305550]
- Rojkind M, Dominguez-Rosales JA, Nieto N, et al. Role of hydrogen peroxide and oxidative stress in healing responses. *Cellular and molecular life sciences : CMLS*. 2002; 59:1872–91. [PubMed: 12530519]
- Varone A, Xylas J, Quinn KP, et al. Endogenous two-photon fluorescence imaging elucidates metabolic changes related to enhanced glycolysis and glutamine consumption in precancerous epithelial tissues. *Cancer Res*. 2014; 74:3067–75. [PubMed: 24686167]
- Zipfel WR, Williams RM, Christie R, et al. Live tissue intrinsic emission microscopy using multiphoton-excited native fluorescence and second harmonic generation. *Proc Natl Acad Sci U S A*. 2003; 100:7075–80. [PubMed: 12756303]

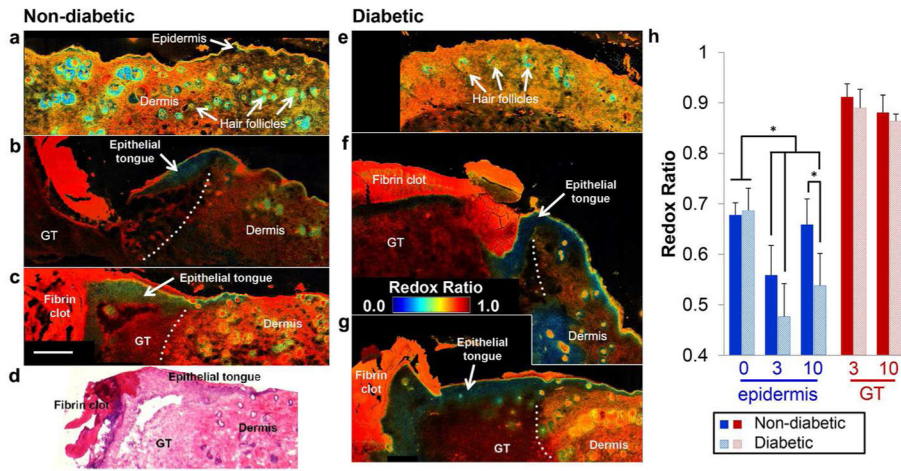


Figure 1.

An optical redox ratio reveals spatial and temporal variability in cell metabolism at the wound edge of non-diabetic (a-c) and diabetic (e-g) mice on Day 0 (a, e), Day 3 (b, f), and Day 10 (c, g) post-wounding. Spatial variability in the redox ratio enables discrimination of wound regions similar to H&E staining (d). Average redox ratios at different time points from the epidermis and granulation tissue (GT) demonstrate significant changes in epithelial metabolism (h). A low redox ratio at Day 3 and thickening of the epithelial tongue by Day 10 is apparent for both groups (b-c, f-g). Dotted lines demarcate the wound edge. The epidermal redox ratio of diabetic wounds remains lower than controls at Day 10 ($p=0.0303$), indicating a delay in the re-epithelialization process. Error bars defined as mean \pm SD, and * $p < 0.05$. Scale bar (= 250 μ m) in (c) applies to all micrographs.